

# Substituent-Mediated Transformation of Polynuclear Gold(I)-Sulfido Complexes—From Pentanuclear to Octadecanuclear Cluster-to-Cluster Transformation

Liang-Liang Yan, Liao-Yuan Yao, Ming-Yi Leung & Vivian Wing-Wah Yam\*

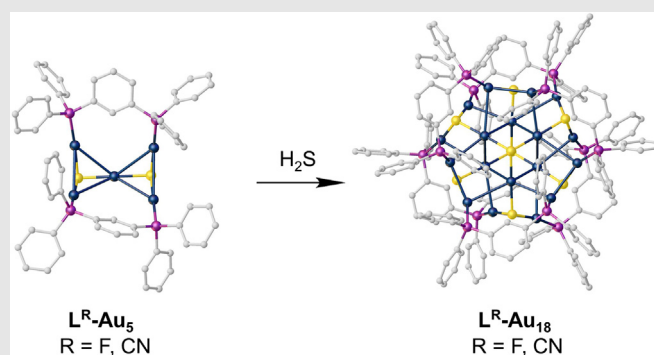
Institute of Molecular Functional Materials and Department of Chemistry, The University of Hong Kong, Pokfulam Road, Hong Kong 999077

\*Corresponding author: [wwyam@hku.hk](mailto:wwyam@hku.hk)

Cite this: CCS Chem. 2021, 3, 326–337

Polynuclear gold complexes show diverse structures and bonding. An exploration into their transformation represents a challenging area of research. Herein, an unprecedented substituent-mediated transformation from pentagold(I) to octadecagold(I) complexes has been observed. These gold(I)-sulfido complexes with distinct structures have been fully characterized, and the transformation process has been monitored by NMR spectroscopy in solution state. The electron-withdrawing effects of the substituent groups on the diphosphine ligands have given rise to subtle changes in the electron density on the gold(I) center, which has resulted in the structural reorganization of the clusters to maximize Au···Au interactions. This compensates for the loss of electron density at the metal center, leading to different symmetries and nuclearities of gold(I)-sulfido complexes with distinctly different photophysical properties. Our findings offer a simple and

effective cluster-to-cluster transformation strategy for the development of novel luminescent gold(I)-sulfido clusters with controlled structures by varying the electronic nature of the substituent on the phosphine ligand.



**Keywords:** supramolecular self-assembly, polynuclear gold(I)-sulfido complexes, substituent-mediated, cluster-to-cluster transformation, electron density

## Introduction

Auophilicity-directed self-assembly has emerged as an effective approach for the construction of diverse architectures.<sup>1–15</sup> In recent decades, growing research interest has focused on the self-assembly of polynuclear gold(I)

aggregates via Au···Au interactions that show strengths similar to that of hydrogen bonding.<sup>16–47</sup> To date, polynuclear gold(I)-sulfido complexes have become a particularly interesting subclass in the gold family due to the comparatively facile synthesis and highly stable structure.<sup>48–56</sup> Recently, our group has made efforts not only to

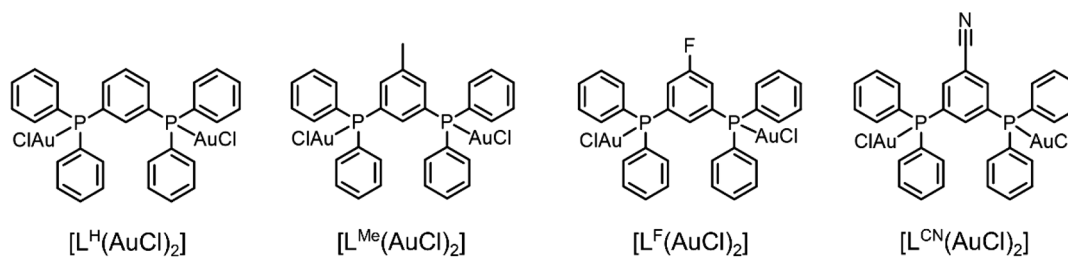


**Chart 1** | Chemical structures of  $[L^H(AuCl)_2]$ ,  $[L^Me(AuCl)_2]$ ,  $[L^F(AuCl)_2]$ , and  $[L^{CN}(AuCl)_2]$ .

build new structures of polynuclear  $\mu_3$ -sulfido gold(I) complexes with rich luminescence properties, but also to study their interesting polynuclear gold(I)-based cluster-to-cluster transformations.<sup>51–54,56</sup> Introducing reactive sites, such as alkynyl groups,<sup>50</sup> vinyl groups,<sup>54</sup> or cis-trans isomerizable groups,<sup>56</sup> to bring about cluster-to-cluster transformation and changes in luminescence properties has led to fascinating structures and properties. However, reactive sites capable of such conversions, while interesting, are rather limited. Thus, a search for a simple but controllable method for the structural regulation of gold(I) clusters is still a major challenge. If the transformation could be extended from the use of specific reactive functional groups to more general ligand design principles, myriad possibilities in the area of transformation would result.

Moreover, ligands with rigid backbones have played important roles in the field of luminescent materials, owing to their abilities of providing extended  $\pi$ -conjugation and molecular rigidity.<sup>57–60</sup> Phosphine ligands with rigid aromatic backbones are widely used in organometallic catalysis and blue phosphorescent organic light-emitting diode materials.<sup>61,62</sup> In polynuclear gold(I)-sulfido complexes, the most commonly used ligands are phosphine ligands with flexible linkers, such as dppm,<sup>52</sup> dpepp,<sup>51</sup> and so on,<sup>50</sup> while ligands based on rigid aromatic skeletons are rarely used. Since the configurations of polynuclear gold(I)-sulfido complexes are sensitive to the P-P bite distances of phosphine ligands, the employment of rigid diphosphine ligands with well-defined P-P bite distances is a feasible and precise way to optimize P-P bite distances for the controlled synthesis of various polynuclear complex structures. Since linear diphosphine ligands  $PPh_2(p\text{-}C_6H_4)_nPPh_2$ , ( $n = 1\text{--}4$ ) have been shown to prefer the formation of supramolecular aggregates ( $n = 1$ ) and cage-like ( $n = 2\text{--}4$ ) structures rather than discrete polynuclear gold(I)-sulfido complexes,<sup>39,40</sup> an exploration in the use of V-shaped ligands based on 1,3-bis(diphenylphosphino)benzene with a shorter P-P bite distance for the assembly of discrete polynuclear gold(I) complexes is worth pursuing. Furthermore, to the best of our knowledge, the role of the substituents of the rigid aromatic skeleton of diphosphine ligands in facilitating the transformation of

the structure of the polynuclear gold(I)-sulfido complexes has rarely been reported.

Herein, we report an interesting finding, in which a minor difference in the substituent group of the rigid diphosphine ligands has resulted in the formation of different structures of the polynuclear gold(I)-sulfido complexes. By employing chlorogold(I) precursors,  $[L^H(AuCl)_2]$ ,  $[L^Me(AuCl)_2]$ ,  $[L^F(AuCl)_2]$ , and  $[L^{CN}(AuCl)_2]$  (Chart 1), a novel series of luminescent polynuclear gold(I)-sulfido complexes,  $[Au_5(L^H)_2S_2]Cl$  ( $[L^H\text{-Au}_5]Cl$ ),  $[Au_5(L^Me)_2S_2]Cl$  ( $[L^Me\text{-Au}_5]Cl$ ),  $[Au_5(L^F)_2S_2]Cl$  ( $[L^F\text{-Au}_5]Cl$ ),  $[Au_{18}(L^F)_6S_8]Cl_2$  ( $[L^F\text{-Au}_{18}]Cl_2$ ),  $[Au_5(L^{CN})_2S_2]Cl$  ( $[L^{CN}\text{-Au}_5]Cl$ ), and  $[Au_{18}(L^{CN})_6S_8]Cl_2$  ( $[L^{CN}\text{-Au}_{18}]Cl_2$ ), have been constructed. These gold(I) complexes have been well characterized. Furthermore, it was found that the electron-withdrawing substituent on the benzene core of 1,3-bis(diphenylphosphino)benzene is of vital importance for the regulation of the cluster transformation process. Intriguingly, the pentagold(I) complexes with electron-withdrawing substituents such as  $-F$  and  $-CN$  were found to transform to octadecagold(I) complexes in solution in the presence of  $H_2S$ . The transformation process has been monitored by NMR spectroscopy. This work not only reveals the transformation process but also provides a simple and convenient strategy to develop controlled transformation for the development of luminescent gold-based materials.

## Experimental Methods

### Synthesis of polynuclear gold(I)-phosphine complexes

#### $[L^H\text{-Au}_5]Cl$

Freshly produced  $H_2S$  gas was bubbled into a solution of  $[L^H(AuCl)_2]$  (91.1 mg, 0.10 mmol) in 11 mL dichloromethane-pyridine (10:1, v/v) at room temperature, resulting in a clear colorless solution. Subsequent evaporation and purification by layering of diethyl ether onto a dichloromethane solution of the complex gave  $[L^H\text{-Au}_5]Cl$  as white crystals. Yield: 53 mg (67% based on the Au content).  $^1H$  NMR (400 MHz,  $CD_2Cl_2$ ),  $\delta$  (ppm): 9.38 (t,  $J = 15.8$  Hz, 1H, phenyl), 7.60–7.32 (m, 17H, phenyl), 7.30–7.19 (m, 2H, phenyl), 7.06–6.86 (m, 4H, phenyl).

$^{31}\text{P}\{\text{H}\}$  NMR (162 MHz,  $\text{CD}_2\text{Cl}_2$ ),  $\delta$  (ppm): 31.5. Positive high-resolution electrospray ionization mass spectrometry (HR-ESI-MS) ( $m/z$ ): calcd for  $[(\text{C}_{30}\text{H}_{24}\text{P}_2)_2\text{Au}_5\text{S}_2]^+$ , 1941.0471; found, 1941.0506. White crystals of  $[\text{L}^{\text{H}}\text{-Au}_5]\text{Cl}$  suitable for X-ray structural determination were obtained by slow vapor diffusion of diethyl ether into a  $\text{CH}_2\text{Cl}_2$  and MeOH mixture (1:1, v/v) solution of  $[\text{L}^{\text{H}}\text{-Au}_5]\text{Cl}$ .

### $[\text{L}^{\text{Me}}\text{-Au}_5]\text{Cl}$

This was prepared according to a procedure similar to that described for  $[\text{L}^{\text{H}}\text{-Au}_5]\text{Cl}$ , except  $[\text{L}^{\text{Me}}(\text{AuCl})_2]$  (93 mg, 0.10 mmol) was used instead. Yield: 58 mg (72% based on the Au content).  $^1\text{H}$  NMR (400 MHz,  $\text{CD}_2\text{Cl}_2$ ),  $\delta$  (ppm): 9.23 (t,  $J = 15.9$  Hz, 1H, phenyl), 7.64–7.18 (m, 18H, phenyl), 7.10–6.84 (m, 4H, phenyl), 2.38 (s, 3H,  $-\text{CH}_3$ ).  $^{31}\text{P}\{\text{H}\}$  NMR (162 MHz,  $\text{CD}_2\text{Cl}_2$ ),  $\delta$  (ppm): 31.3. Positive HR-ESI-MS ( $m/z$ ): calcd for  $[(\text{C}_{31}\text{H}_{26}\text{P}_2)_2\text{Au}_5\text{S}_2]^+$ , 1969.0784; found, 1969.0712.

### $[\text{L}^{\text{F}}\text{-Au}_5]\text{Cl}$

This was prepared according to a procedure similar to that described for  $[\text{L}^{\text{H}}\text{-Au}_5]\text{Cl}$ , except  $[\text{L}^{\text{F}}(\text{AuCl})_2]$  (93 mg, 0.10 mmol) was used instead. Yield: 85 mg (84% based on the Au content).  $^1\text{H}$  NMR (400 MHz,  $\text{CDCl}_3$ ),  $\delta$  (ppm): 9.10 (t,  $J = 15.2$  Hz, 1H, phenyl), 7.55–7.29 (m, 16H, phenyl), 7.12–6.97 (m, 6H, phenyl).  $^{31}\text{P}\{\text{H}\}$  NMR (162 MHz,  $\text{CDCl}_3$ ),  $\delta$  (ppm): 30.4.  $^{19}\text{F}\{\text{H}\}$  NMR (376 MHz,  $\text{CDCl}_3$ ),  $\delta$  (ppm): -106.4. Positive HR-ESI-MS ( $m/z$ ): calcd for  $[(\text{C}_{30}\text{H}_{23}\text{FP}_2)_2\text{Au}_5\text{S}_2]^+$ , 1977.0282; found, 1977.0137. White crystals of  $[\text{L}^{\text{F}}\text{-Au}_5]\text{Cl}$  suitable for X-ray structural determination were obtained by slow vapor diffusion of diethyl ether into a  $\text{CH}_2\text{Cl}_2$  and MeOH mixture (1:1, v/v) solution of  $[\text{L}^{\text{F}}\text{-Au}_5]\text{Cl}$ .

### $[\text{L}^{\text{CN}}\text{-Au}_5]\text{Cl}$

Freshly produced  $\text{H}_2\text{S}$  gas was bubbled into a solution of  $[\text{L}^{\text{CN}}(\text{AuCl})_2]$  (46.8 mg, 0.05 mmol) in dichloromethane-pyridine (22 mL, 10:1, v/v) at room temperature, resulting in a clear solution in 5 min. Subsequent evaporation and purification by layering diethyl ether onto a dichloromethane solution of the complex gave  $[\text{L}^{\text{CN}}\text{-Au}_5]\text{Cl}$  as a white solid. Yield: 23.1 mg (57% based on the Au content).  $^1\text{H}$  NMR (400 MHz,  $\text{CD}_2\text{Cl}_2$ ),  $\delta$  (ppm): 9.41 (t,  $J = 14.9$  Hz, 1 H, phenyl), 7.80–7.30 (m, 18H, phenyl), 7.30–7.00 (m, 4H, phenyl).  $^{31}\text{P}\{\text{H}\}$  NMR (162 MHz,  $\text{CD}_2\text{Cl}_2$ ),  $\delta$  (ppm): 31.5. Positive HR-ESI-MS ( $m/z$ ): calcd for  $[(\text{C}_{31}\text{H}_{23}\text{NP}_2)_2\text{Au}_5\text{S}_2]^+$ , 1991.0376; found, 1991.0417.

### $[\text{L}^{\text{F}}\text{-Au}_{18}]\text{Cl}_2$

Freshly produced  $\text{H}_2\text{S}$  gas was bubbled into a solution of  $[\text{L}^{\text{F}}(\text{AuCl})_2]$  (186 mg, 0.20 mmol) in dichloromethane-pyridine (11 mL, 10:1, v/v) at room temperature, resulting in a clear colorless solution in 10 min. Further bubbling of

$\text{H}_2\text{S}$  gas for 5 h, followed by evaporation of the solvent and recrystallization from dichloromethane solution gave  $[\text{L}^{\text{F}}\text{-Au}_{18}]\text{Cl}_2$  as yellow tetrahedron-shaped crystals. Yield: 78 mg (53% based on the Au content).  $^1\text{H}$  NMR (400 MHz,  $\text{CD}_2\text{Cl}_2$ ),  $\delta$  (ppm): 9.83 (t,  $J = 14.2$  Hz, 1H, phenyl), 7.81–6.22 (m, 22H, phenyl).  $^{31}\text{P}\{\text{H}\}$  NMR (162 MHz,  $\text{CD}_2\text{Cl}_2$ ),  $\delta$  (ppm): 29.4.  $^{19}\text{F}\{\text{H}\}$  NMR (376 MHz,  $\text{CD}_2\text{Cl}_2$ ),  $\delta$  (ppm): -110.24. Positive HR-ESI-MS ( $m/z$ ): calcd for  $[(\text{C}_{30}\text{H}_{23}\text{FP}_2)_6\text{Au}_{18}\text{S}_8]^{2+}$ , 3293.9670; found, 3293.9475. Yellow crystals of  $[\text{L}^{\text{F}}\text{-Au}_{18}]\text{Cl}_2$  suitable for X-ray structural determination were obtained by slow vapor diffusion of diethyl ether into a dichloromethane solution of  $[\text{L}^{\text{F}}\text{-Au}_{18}]\text{Cl}_2$ .

### $[\text{L}^{\text{CN}}\text{-Au}_{18}]\text{Cl}_2$

Freshly produced  $\text{H}_2\text{S}$  gas was bubbled into a solution of  $[\text{L}^{\text{CN}}(\text{AuCl})_2]$  (46.8 mg, 0.05 mmol) in dichloromethane-pyridine (22 mL, 10:1, v/v) at room temperature, resulting in a clear red solution in 10 min. Further bubbling of  $\text{H}_2\text{S}$  gas for 1 h, followed by evaporation of the solvent and recrystallization from slow vapor diffusion of diethyl ether into a dichloromethane solution gave  $[\text{L}^{\text{CN}}\text{-Au}_{18}]\text{Cl}_2$  as red crystals, suitable for X-ray structural determination. Yield: 15.1 mg (41% based on the Au content).  $^1\text{H}$  NMR (400 MHz,  $\text{CD}_2\text{Cl}_2$ ),  $\delta$  (ppm): 10.00 (t,  $J = 13.5$  Hz, 1H, phenyl), 7.61–7.23 (m, 14H, phenyl), 7.18 (d,  $J = 8.5$  Hz, 2H, phenyl), 7.02–6.89 (m, 2H, phenyl). 6.58–6.40 (m, 4H, phenyl).  $^{31}\text{P}\{\text{H}\}$  NMR (162 MHz,  $\text{CD}_2\text{Cl}_2$ ),  $\delta$  (ppm): 30.3. Positive HR-ESI-MS ( $m/z$ ): calcd for  $[(\text{C}_{31}\text{H}_{23}\text{NP}_2)_6\text{Au}_{18}\text{S}_8]^{2+}$ , 3314.9810; found, 3314.9650.

## Results and Discussion

### Synthesis and characterization

A series of pentanuclear and octadecanuclear gold(I)-sulfido complexes, denoted as  $[\text{L}^{\text{H}}\text{-Au}_5]\text{Cl}$ ,  $[\text{L}^{\text{Me}}\text{-Au}_5]\text{Cl}$ ,  $[\text{L}^{\text{F}}\text{-Au}_5]\text{Cl}$ ,  $[\text{L}^{\text{CN}}\text{-Au}_5]\text{Cl}$ ,  $[\text{L}^{\text{F}}\text{-Au}_{18}]\text{Cl}_2$ , and  $[\text{L}^{\text{CN}}\text{-Au}_{18}]\text{Cl}_2$ , were synthesized by bubbling  $\text{H}_2\text{S}$  into a dichloromethane-pyridine mixture of respective chlorogold(I) precursors. All polynuclear gold(I) complexes were characterized by NMR, HR-ESI-MS, and electronic absorption and emission spectroscopies (Supporting Information Figures S1–S21). The  $^{31}\text{P}\{\text{H}\}$  NMR spectrum of  $[\text{L}^{\text{H}}\text{-Au}_5]\text{Cl}$  in  $\text{CD}_2\text{Cl}_2$  shows only one singlet at  $\delta = 31.5$  ppm (Supporting Information Figure S3), indicating that the two phosphorus atoms of  $\text{L}^{\text{H}}$  are in the same environment. The other pentanuclear gold(I)-sulfido complexes show similar  $^{31}\text{P}\{\text{H}\}$  NMR spectra (Supporting Information Figures S5, S7, and S13), suggesting that the structures of these  $\text{Au}_5$  complexes are similar to phosphorus atoms in the same environment. Upon diffusion of diethyl ether vapor into a concentrated solution of  $[\text{L}^{\text{H}}\text{-Au}_5]\text{Cl}$  in  $\text{CH}_2\text{Cl}_2$  and MeOH (1:1, v/v) mixture, single crystals of  $[\text{L}^{\text{H}}\text{-Au}_5]\text{Cl}$  were obtained. Single-crystal X-ray diffraction analysis further confirms

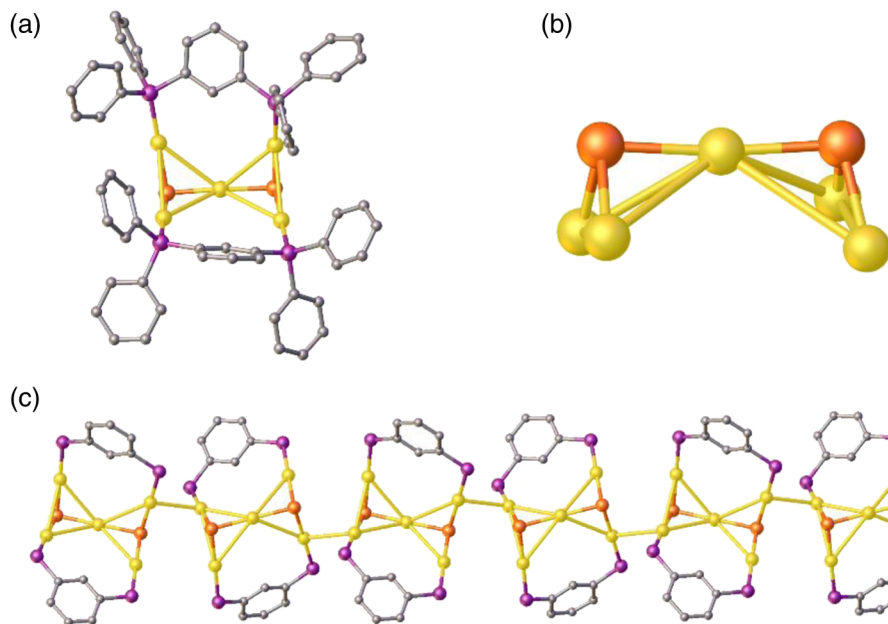


**Figure 1** | (a) Crystal structure of  $[L^H\text{-Au}_5]\text{Cl}$ . (b) Core of the crystal structure of  $[L^H\text{-Au}_5]\text{Cl}$ . (c) Packing of linear 1-D molecular arrays in the crystal structure of  $[L^H\text{-Au}_5]\text{Cl}$  (gray, C; purple, P; yellow, Au; orange, S).

the formation of  $[L^H\text{-Au}_5]\text{Cl}$ , which crystallizes in the monoclinic  $P2_1$  space group ([Supporting Information Table S1](#)). The five gold(I) atoms are surrounded by two nearly trans-disposed diphosphine ligands ([Figures 1a](#), [1b](#) and [Supporting Information Figures S22](#)) and bridged by two  $\mu_3\text{-S}$  atoms with Au-S-Au angles in the range of 86.87–96.53° ([Supporting Information Table S3](#)). The Au…Au distances range from 3.08 to 3.37 Å, which are in the normal range for aurophilic interactions ([Supporting Information Table S2](#)). More interestingly, the discrete complex  $[L^H\text{-Au}_5]\text{Cl}$  can further assemble to form one-dimensional linear supramolecular aggregates via intermolecular gold…gold interactions in the crystalline state ([Figure 1c](#)).  $\text{Cl}^-$  counterions were found to be located around the phosphine ligand with hydrogen-bonding distances ranging from 2.66–3.24 Å ([Supporting Information Figure S23](#)). This represents the first example of the crystal structure of pentanuclear gold (I)-sulfido complex based on diphosphine ligands. There is no symmetry in the solid state observed in the single-crystal structure determination. However, only one P environment is observed in the  $^{31}\text{P}\{\text{H}\}$  NMR spectrum ([Supporting Information Figure S3](#)), suggesting a local  $C_{2v}$  symmetry of  $[L^H\text{-Au}_5]\text{Cl}$  in the solution state. Similarly, single crystals of  $[L^F\text{-Au}_5]\text{Cl}$  have also been obtained under the same conditions. The related information of the crystal structure data is summarized in [Supporting Information Tables S4–S6](#) and [Figure S24](#).

Interestingly, with exposure to  $\text{H}_2\text{S}$  atmosphere overnight, the solution colors of  $[L^F\text{-Au}_5]\text{Cl}$  and  $[L^{\text{CN}}\text{-Au}_5]\text{Cl}$  slowly change from colorless to yellow and red, respectively. However, similar phenomena are not observed for

the solutions of  $[L^H\text{-Au}_5]\text{Cl}$  and  $[L^{\text{Me}}\text{-Au}_5]\text{Cl}$  under similar conditions. The yellow complex product,  $[L^F\text{-Au}_{18}]\text{Cl}_2$ , has been isolated as tetrahedron-shaped crystals by the diffusion of diethyl ether into the dichloromethane solution, which was found to be suitable for single-crystal X-ray diffraction analysis. The single-crystal X-ray structure shows that  $[L^F\text{-Au}_{18}]\text{Cl}_2$  is  $[\text{Au}_{18}(L^F)_6(\mu_3\text{-S})_8]^{2+}$  ( $[L^F\text{-Au}_{18}]^{2+}$ ) ([Figure 2a](#)). The crystal structure of  $[L^F\text{-Au}_{18}]\text{Cl}_2$  is refined in the cubic  $\bar{I}\bar{4}3d$  space group ([Supporting Information Tables S7–S9](#)). Intriguingly, the F…F distance between every two adjacent  $\text{Au}_{18}$  complexes in the crystal structure is shown to be 2.94 Å ([Figure 2c](#)), suggesting the presence of F…F interactions, which helps to stabilize crystal packing.<sup>63</sup> The complex cation  $[L^F\text{-Au}_{18}]\text{Cl}_2$  is comprised of six diphosphine ligands, eighteen gold(I) atoms, and eight  $\mu_3$ -bridging S atoms ([Figure 2a](#)) to give an octadecanuclear gold(I)-sulfido cluster structure, which is similar to the related  $\text{Au}_{18}$  clusters,  $[\text{Au}_{18}\text{Se}_8(\text{dppe})_6]^{2+}$ ,<sup>21</sup>  $[\text{Au}_{18}\text{S}_8(\text{dppe})_6]^{2+}$ ,<sup>64</sup> and  $[\text{Au}_{18}\text{S}_8(\mu\text{-trans-dppee})_3]^{2+}$ .<sup>56</sup> The gold skeleton of  $[L^F\text{-Au}_{18}]\text{Cl}_2$  consists of a peripheral  $\text{Au}_{12}$  macrocycle linked by Au…Au and Au–S interactions ([Figure 2b](#)) and the kernel of the gold skeleton can be viewed as a twisted cube consisting of a  $\text{Au}_6\text{S}_2$  core ([Figure 2a](#)). The Au…Au contacts range from 2.95 to 3.27 Å, which are in the range of aurophilic interactions ([Supporting Information Table S8](#)). Also, in the  $^{31}\text{P}\{\text{H}\}$  NMR spectrum of  $[L^F\text{-Au}_{18}]\text{Cl}_2$ , only one singlet at  $\delta = 29.4$  ppm was found, suggesting that two phosphorus atoms on the same ligand are equivalent ([Supporting Information Figure S10](#)). The identity of  $[L^F\text{-Au}_{18}]\text{Cl}_2$  was further confirmed by HR-ESI-MS analyses. A prominent cluster peak at

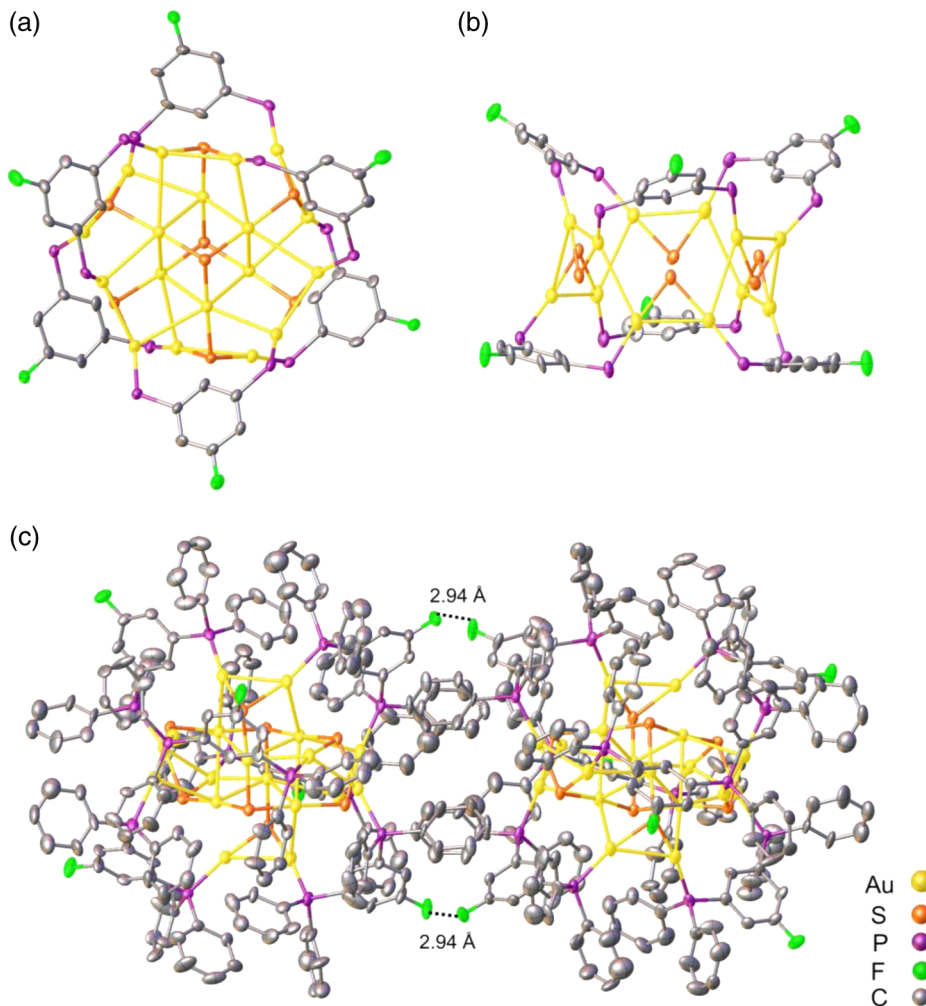


**Figure 2** | (a) Perspective view of  $[L^F\text{-}\text{Au}_{18}]Cl_2$ . (b) Side view of peripheral  $\text{Au}_{12}$  macrocycle skeleton in  $[L^F\text{-}\text{Au}_{18}]Cl_2$ . (c) Packing of adjacent molecules in the crystal structure of  $[L^F\text{-}\text{Au}_{18}]Cl_2$ . Thermal ellipsoids are shown at a 50% probability level. The counteranions, solvent molecules, and hydrogen atoms are omitted for clarity (gray, C; green, F; purple, P; yellow, Au; orange, S).

$m/z = 3293.95$  can be attributed to the doubly charged molecular ion cluster,  $[\text{Au}_{18}(L^F)_6\text{S}_8]^{2+}$ , with the loss of  $\text{Cl}^-$  counterions. This assignment is supported by the good agreement of the simulated isotopic pattern of the ion cluster with the high-resolution experimental MS isotopic pattern (Supporting Information Figure S19). The  $^1\text{H}$  and  $^{19}\text{F}\{\text{H}\}$  NMR spectral data also support the assignment (Supporting Information Figures S9 and S11). Similarly, NMR, HR-ESI-MS spectroscopy, and single-crystal X-ray diffraction studies have also been used to establish the structure of  $[L^{\text{CN}}\text{-}\text{Au}_{18}]Cl_2$  (Supporting Information Tables S10-S12, Figures S14, S15, S21, and S25), indicating that the structure of  $[L^{\text{CN}}\text{-}\text{Au}_{18}]Cl_2$  is similar to that of  $[L^F\text{-}\text{Au}_{18}]Cl_2$ .

### Photophysical studies

A cluster-to-cluster conversion from  $\text{Au}_5$  to  $\text{Au}_{18}$  has brought about a dramatic red shift in the UV-vis

absorption spectra (Supporting Information Figure S1). The UV-vis absorption spectra of these pentanuclear and octadecanuclear gold(I)-sulfido clusters show low-energy absorption shoulders at 320 and 400 nm, respectively (Supporting Information Figure S1), which are absent in the chlorogold(I) precursors and are tentatively assigned as ligand-to-metal-metal charge transfer (LMMCT;  $S \rightarrow \text{Au}_n$ ) or ligand-to-metal charge transfer (LMCT;  $S \rightarrow \text{Au}$ ) transitions modified by  $\text{Au(I)}\cdots\text{Au(I)}$  interactions. The red shift may be due to the increase in nuclearity from pentanuclear to octadecanuclear and the shorter  $\text{Au}\cdots\text{Au}$  distances observed in octadecanuclear clusters that narrow the highest occupied molecular orbital (HOMO)-lowest unoccupied molecular orbital (LUMO) energy gap. The luminescent properties of the complexes were found to be different, and the pentanuclear clusters are nonemissive in solution. It is possible that the open structure and fluxionality of pentanuclear clusters allow their emission to be readily quenched by

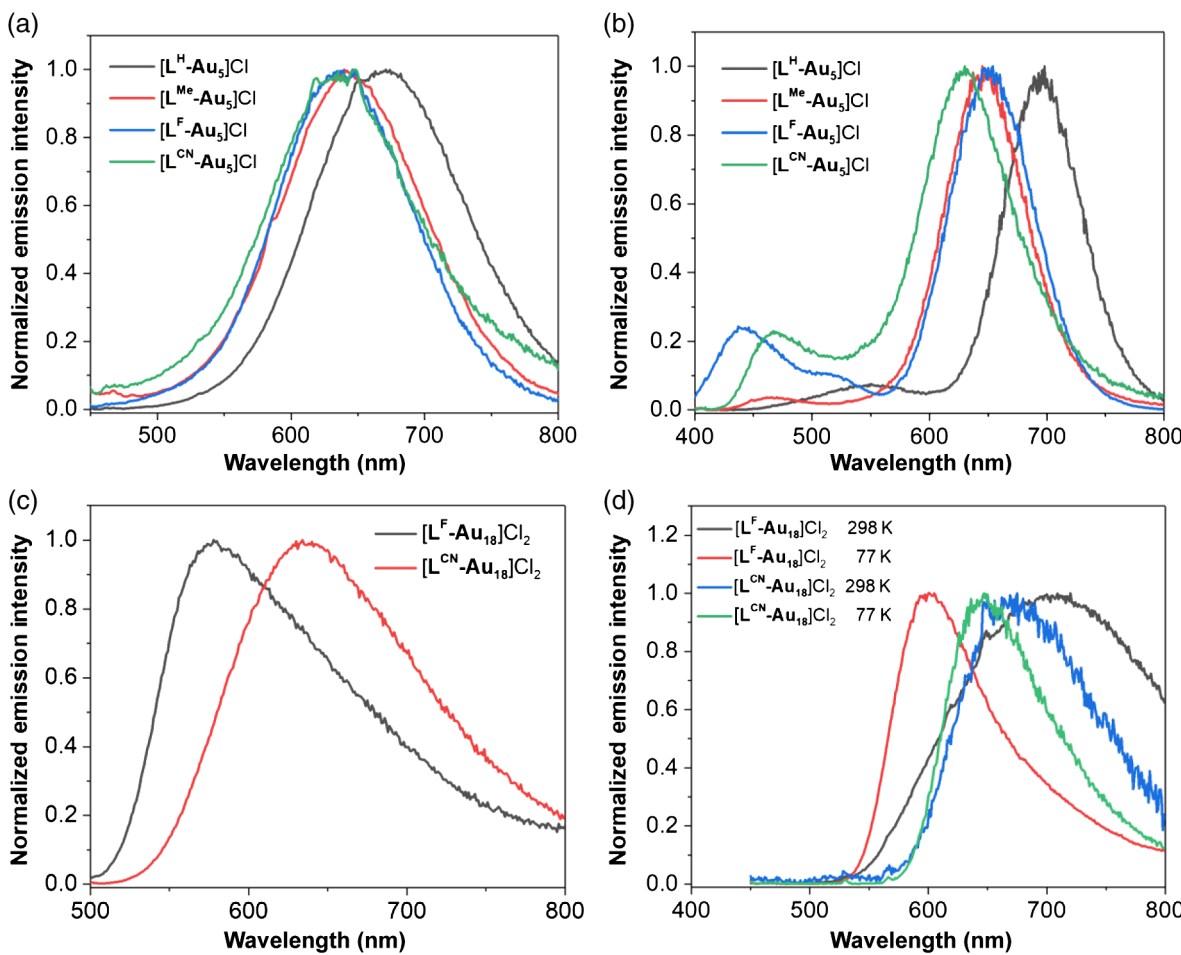


**Figure 3** | Solid-state emission spectra of  $[L^H\text{-Au}_5]\text{Cl}$ ,  $[L^{\text{Me}}\text{-Au}_5]\text{Cl}$ ,  $[L^F\text{-Au}_5]\text{Cl}$ , and  $[L^{\text{CN}}\text{-Au}_5]\text{Cl}$  (a) at room temperature and (b) low temperature (77 K). (c) Solution-state emission spectra of  $[L^F\text{-Au}_{18}]\text{Cl}_2$  and  $[L^{\text{CN}}\text{-Au}_{18}]\text{Cl}_2$  in dichloromethane. (d) Solid-state emission spectra of  $[L^F\text{-Au}_{18}]\text{Cl}_2$  and  $[L^{\text{CN}}\text{-Au}_{18}]\text{Cl}_2$  at room temperature and low temperature (77 K).

solvent and molecular motion. However, they emit red light in the solid state at ambient temperature with photoluminescence quantum yield (PLQY) up to around 10.8% (Figure 3a and Table 1), possibly attributable to the rigid environment exerted by the rigid ligands in the solid lattice. These pentanuclear clusters show a dual blue-green and orange-red luminescence in the solid state at 77 K (Figure 3b). In contrast, the octadecanuclear clusters not only are emissive in dichloromethane with PLQY of up to around 3.7% in solution (Figure 3c and Table 1), but also give an orange-red emission in the solid state at room temperature upon excitation with PLQY up to around 6.0% (Figure 3d and Table 1). The low-energy emission bands for these complexes near 570–710 nm can be assigned as arising from  ${}^3\text{LMMCT}$  excited-state origin or  ${}^3\text{LMCT}$  excited-state origin modified by metal...metal interactions, while the high-energy blue-green emission bands can be assigned as arising from the metal-perturbed ligand-centered phosphorescence, similar to that reported in previous studies.<sup>65</sup>

## Study of the transformation process

To better understand the mechanism of cluster-to-cluster transformation, the assembly process has been monitored by  ${}^1\text{H}$ ,  ${}^{31}\text{P}\{{}^1\text{H}\}$ , and  ${}^{19}\text{F}\{{}^1\text{H}\}$  NMR spectroscopies in  $\text{CDCl}_3$ -pyridine (10:1 v/v) (Figure 4). The signal of the proton ( $\text{H}_A$ ) in the ligand backbone between the two phosphorus atoms has been monitored (Figure 4a). As shown in Figure 3b, the initial proton signal in the precursor  $[L^F(\text{AuCl})_2]$  occurs at around  $\delta = 7.05$  ppm. Continuous bubbling of  $\text{H}_2\text{S}$  for around 5 min has led to the appearance of a new and broad signal around  $\delta = 9.12$  ppm. Meanwhile, the disappearance of the  ${}^{19}\text{F}$  and  ${}^{31}\text{P}$  signals of the  $[L^F(\text{AuCl})_2]$  precursor and the appearance of the new signals of  $[L^F\text{-Au}_5]\text{Cl}$  at around  $\delta = -106.50$  and 30.50 ppm can unambiguously confirm the complete consumption of the precursor, giving only  $[L^F\text{-Au}_5]\text{Cl}$  in solution (Figures 4d and 4e). As the reaction proceeded for approximately 30 min, another proton signal at  $\delta = 9.83$  ppm attributed to the proton of

**Table 1 | Photophysical Properties of Complexes**

Complex	Media ( <i>T</i> [K])	UV-vis $\lambda_{\text{max}}$ (nm) ( $\epsilon \times 10^{-5}$ [ $\text{dm}^3\text{mol}^{-1}\text{cm}^{-1}$ ])	Emission $\lambda_{\text{em}}$ (nm)	Emission Quantum Yield (%) <sup>a</sup>
[L <sup>H</sup> -Au <sub>5</sub> ]Cl	CH <sub>2</sub> Cl <sub>2</sub> (298)	287 sh (0.09)	— <sup>b</sup>	— <sup>b</sup>
	Solid (298)		668	~10.8
	Solid (77)		550, 695	
[L <sup>Me</sup> -Au <sub>5</sub> ]Cl	CH <sub>2</sub> Cl <sub>2</sub> (298)	293 sh (0.17)	— <sup>b</sup>	— <sup>b</sup>
	Solid (298)		644	~7.4
	Solid (77)		465, 646	
[L <sup>F</sup> -Au <sub>5</sub> ]Cl	CH <sub>2</sub> Cl <sub>2</sub> (298)	293 sh (0.13)	— <sup>b</sup>	— <sup>b</sup>
	Solid (298)		651	~7.7
	Solid (77)		440, 650	
[L <sup>CN</sup> -Au <sub>5</sub> ]Cl	CH <sub>2</sub> Cl <sub>2</sub> (298)	289 sh (0.08)	— <sup>b</sup>	— <sup>b</sup>
	Solid (298)		633	~1.9
	Solid (77)		469, 629	
[L <sup>F</sup> -Au <sub>18</sub> ]Cl <sub>2</sub>	CH <sub>2</sub> Cl <sub>2</sub> (298)	390 sh (0.16)	580	~2.0
	Solid (298)		705	~5.7
	Solid (77)		600	
[L <sup>CN</sup> -Au <sub>18</sub> ]Cl <sub>2</sub>	CH <sub>2</sub> Cl <sub>2</sub> (298)	384 sh (0.22)	637	~3.7
	Solid (298)		670	~6.0
	Solid (77)		645	

<sup>a</sup> Solution emission quantum yields were measured with reference to [Ru(bpy)<sub>3</sub>]Cl<sub>2</sub> in H<sub>2</sub>O.

<sup>b</sup> No emission was detected for complexes in dichloromethane solution.

[L<sup>F</sup>-Au<sub>18</sub>]Cl<sub>2</sub> emerged. The formation of [L<sup>F</sup>-Au<sub>18</sub>]Cl<sub>2</sub> can also be observed in the <sup>19</sup>F{<sup>1</sup>H} and <sup>31</sup>P{<sup>1</sup>H} NMR spectra, such as a new signal at  $\delta = 29.1$  ppm in the <sup>31</sup>P{<sup>1</sup>H} NMR spectra and a new signal at  $\delta = -109.1$  ppm in the <sup>19</sup>F{<sup>1</sup>H} NMR spectra assigned to [L<sup>F</sup>-Au<sub>18</sub>]Cl<sub>2</sub> (Figures 4c and 4d). As the reaction proceeds, the colorless solution turns yellow (Figure 4e) and signals characteristics of [L<sup>F</sup>-Au<sub>5</sub>]Cl disappear; meanwhile that of [L<sup>F</sup>-Au<sub>18</sub>]Cl<sub>2</sub> are growing in intensity (Figures 4b–4d). Finally, after 2 h, only the signals of [L<sup>F</sup>-Au<sub>18</sub>]Cl<sub>2</sub> can be observed in solution, indicating the completion of the transformation process.<sup>a</sup> Similarly, the cluster-to-cluster transformation process has also been confirmed by HR-ESI-MS (Supporting Information Figure S26). The control experiments involving the mixing of [L<sup>F</sup>-Au<sub>5</sub>]Cl with excess acetic acid or pyridine, respectively, do not lead to similar observations (Supporting Information Figures S27–S30). It is likely that the acid and base do not play a key role in cluster-to-cluster transformation. In addition, the S to Au atomic ratio in [L<sup>F</sup>-Au<sub>5</sub>]Cl was 1:2.5, which is smaller than 1:2.25 in [L<sup>F</sup>-Au<sub>18</sub>]Cl<sub>2</sub>. It is suggested that the H<sub>2</sub>S could provide the necessary S source of the reaction. Further control experiments involving the mixing of [L<sup>F</sup>(AuCl)<sub>2</sub>] with different ratios of Li<sub>2</sub>S confirm the hypothesis (Supporting Information Figure S31). [L<sup>F</sup>-Au<sub>5</sub>]Cl was found to transform to [L<sup>F</sup>-Au<sub>18</sub>]Cl<sub>2</sub> with increasing ratios of Li<sub>2</sub>S.

The Au<sub>3</sub>S unit is the smallest building block in the gold(I)  $\mu_3$ -sulfido clusters. Given that the distance

between the two gold atoms in [L<sup>F</sup>-Au<sub>5</sub>]Cl is 5.03 Å, which is about twice the length of the Au-S bond (Figure 5a), it is rather conducive for [L<sup>F</sup>-Au<sub>5</sub>]Cl to be formed initially within the first 5 min. With time, [L<sup>F</sup>-Au<sub>5</sub>]Cl is transformed into [L<sup>F</sup>-Au<sub>18</sub>]Cl<sub>2</sub>, which has a larger number of Au...Au contacts, as well as Au-S bonds, and relatively shorter Au...Au distances, providing [L<sup>F</sup>-Au<sub>18</sub>]Cl<sub>2</sub> its thermodynamic stability. The rearrangement of the diphosphine ligands has led to the reconfiguration of the cluster structures. It was found that the diphosphine ligands and two gold atoms lie nearly on the same plane in the single-crystal structure of [L<sup>F</sup>-Au<sub>5</sub>]Cl, indicating that the lone pairs on the two P atoms also lie on the same plane as the ligand (Figure 5b), with the distance of the two P atoms 5.53 Å apart, bringing the two gold atoms to a separation of 5.03 Å (Figure 5a); while in [L<sup>F</sup>-Au<sub>18</sub>]Cl<sub>2</sub>, the separations of the two P atoms and the two gold atoms were 5.49 and 5.96 Å, respectively (Figure 5a). Compared with [L<sup>F</sup>-Au<sub>5</sub>]Cl, the distance between the two gold atoms in [L<sup>F</sup>-Au<sub>18</sub>]Cl<sub>2</sub> is 0.93 Å longer and the two gold atoms are deviated from the plane of the ligand (Figure 5). It is a result of the rotation of the C-P bond, which renders the lone pairs on the two P atoms pointing toward a direction out of the plane. Such rearrangement of the diphosphine ligands affects the initial weaker aurophilic interactions to maximize the gold(I)...gold(I) interactions with increasing reaction time, resulting in the transformation of the cluster from [L<sup>F</sup>-Au<sub>5</sub>]Cl to more stable [L<sup>F</sup>-Au<sub>18</sub>]Cl<sub>2</sub> units.

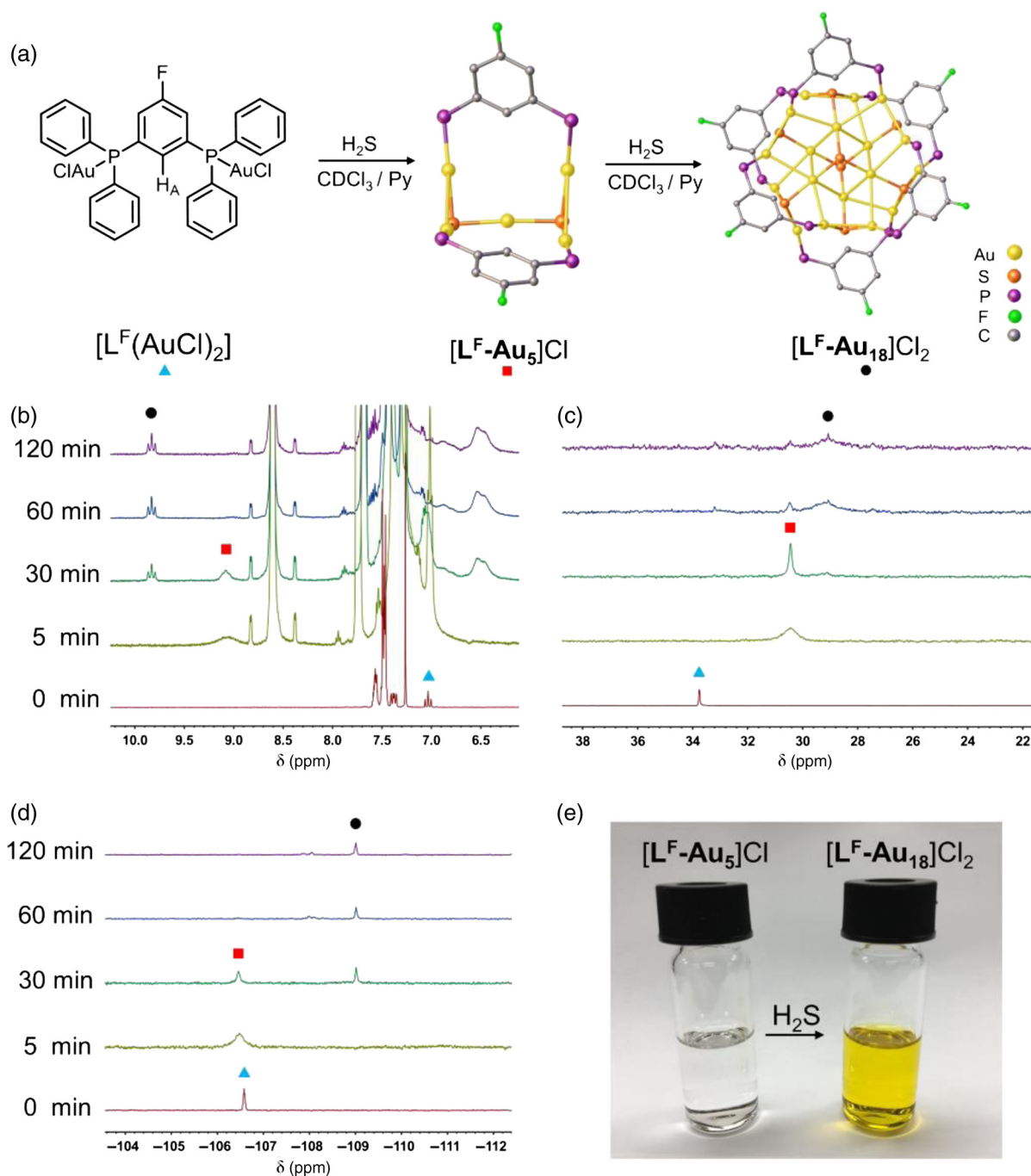


**Figure 4 |** (a) Self-assembly and transformation process of polynuclear gold(I) complexes (other ligands, counter-anions, and hydrogen atoms are omitted for clarity). (b)  $^1\text{H}$  NMR, (c)  $^{31}\text{P}\{^1\text{H}\}$  NMR, and (d)  $^{19}\text{F}\{^1\text{H}\}$  NMR spectral changes and (e) solution color changes in  $\text{CDCl}_3$  during the assembly process (gray, C; green, F; purple, P; yellow, Au; orange, S).

However, similar transformation processes cannot be found in the other two  $\text{Au}_5$  complexes ( $[\text{L}^{\text{H}}\text{-Au}_5]\text{Cl}$  and  $[\text{L}^{\text{Me}}\text{-Au}_5]\text{Cl}$ ) under the same conditions. It is suggested that the electron-withdrawing substituents (such as  $-\text{F}$  and  $-\text{CN}$ ) on the rigid skeleton of the diphosphine ligand may be a key factor in the cluster transformation. With reference to our previous works on gold(I)-phosphine complexes,<sup>66,67</sup> it is likely that the more electron-

withdrawing substituent groups on the diphosphine ligands would lead to reduced electron densities at the gold(I) centers that induce a structural reorganization of the clusters ( $[\text{L}^{\text{F}}\text{-Au}_{18}]\text{Cl}_2$  and  $[\text{L}^{\text{CN}}\text{-Au}_{18}]\text{Cl}_2$ ) to compensate for the loss of electron density at the gold(I) centers through an increase in the number of  $\text{Au}\cdots\text{Au}$  contacts as well as an enhancement of the  $\text{Au}\cdots\text{Au}$  interactions. The reduction in electron density at the gold(I) centers by the

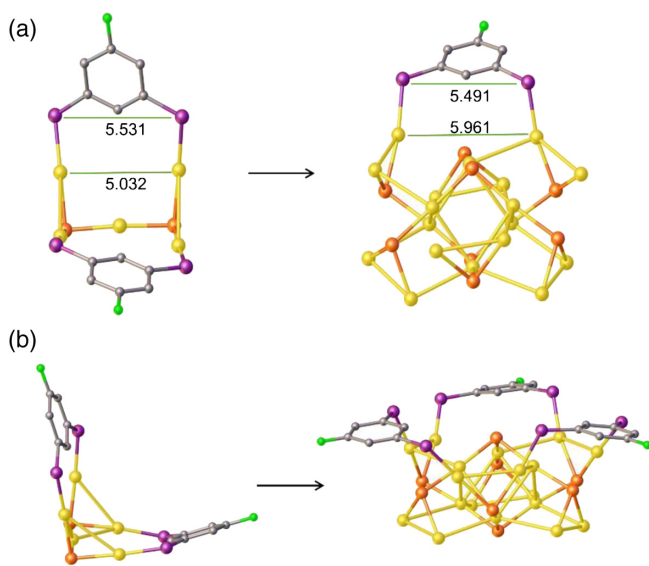


**Figure 5 |** (a) Bridging models and (b) side view of bridging models in the solid state; selected distances are shown. Other ligands, counteranions, and hydrogen atoms are omitted for clarity (gray, C; green, F; purple, P; yellow, Au; orange, S).

electron-withdrawing substituent groups on the diphosphine ligands has also been supported by density functional theory (DFT) calculations ([Supporting Information Figures S32–S41](#)).

## Conclusions

An unprecedented cluster-to-cluster transformation from  $\text{Au}_5$  to  $\text{Au}_{18}$  is reported in this work. The self-assembly and transformation processes have been monitored by  $^1\text{H}$ ,  $^{31}\text{P}$  { $^1\text{H}$ }, and  $^{19}\text{F}$ { $^1\text{H}$ } NMR spectroscopies and revealed by single-crystal structural analysis combined with UV-vis absorption and emission spectroscopies. The subtle changes in the electron density on the gold(I) center have resulted in different reorganization abilities of the clusters. Such a significant conversion of the nuclearity of gold(I) clusters has resulted in different photophysical behaviors. This work has provided a new way of exploring cluster-to-cluster transformation, which can control structural reorganization by changing the electronic nature of the substituents of the ligand. Further work in our laboratory on modulating the structures of gold(I) clusters with various bridging ligands is in progress.

## Footnote

<sup>a</sup> Upon monitoring the transformation process, there are some signals in the  $^{19}\text{F}$ { $^1\text{H}$ } and  $^{31}\text{P}$ { $^1\text{H}$ } NMR spectra that cannot be identified. Attempts to identify the byproducts using HR-ESI-MS were not successful, probably due to the difficulty in the ionization of these unidentifiable species.

## Supporting Information

Supporting Information is available and includes general, synthesis and characterization, X-ray crystallography, photophysical studies, computational details, and supplementary figures.

## Conflict of Interest

There are no conflicts of interest to report.

## Acknowledgments

V.W.-W.Y. acknowledges UGC funding administered by The University of Hong Kong for supporting the Electrospray Ionization Quadrupole Time-of-Flight Mass Spectrometry Facilities under the Support for Interdisciplinary Research in Chemical Science and the support from The University of Hong Kong under the University Research Committee (URC) Strategically Oriented Research Theme on Functional Materials for Molecular Electronics. This work has been supported by the Key Program of the Major Research Plan on “Architectures, Functionalities and Evolution of Hierarchical Clusters” of the National Natural Science Foundation of China (grant no. 91961202) and a General Research Fund (GRF) from the Research Grants Council of Hong Kong Special Administrative Region, China (HKU17301517). L.-L.Y. acknowledges the receipt of a postgraduate studentship from The University of Hong Kong. The Beijing Synchrotron Research Facility (BSRF) is also acknowledged for providing beamline time of the synchrotron radiation X-ray diffraction facilities. The authors also thank the staff of BL17B beamline at the National Facility for Protein Science (NFPS) of the Shanghai Synchrotron Radiation Facility, China, for assistance during data collection. The computations were performed using research computing facilities offered by the Information Technology Services at HKU. Dr. Maggie Ng is thanked for her valuable discussions and assistance in the computational studies.

## References

1. Che, C.-M.; Lai, S.-W. Structural and Spectroscopic Evidence for Weak Metal-Metal Interactions and Metal-Substrate Exciplex Formations in  $d^{10}$  Metal Complexes. *Coord. Chem. Rev.* **2005**, *249*, 1296–1309.
2. Fernando, A.; Weerawardene, K. L. D. M.; Karimova, N. V.; Aikens, C. M. Quantum Mechanical Studies of Large Metal, Metal Oxide, and Metal Chalcogenide Nanoparticles and Clusters. *Chem. Rev.* **2015**, *115*, 6112–6216.
3. Gimeno, M. C.; Laguna, A. Three- and Four-Coordinate Gold(I) Complexes. *Chem. Rev.* **1997**, *97*, 511–522.
4. Gimeno, M. C.; Laguna, A. Chalcogenide Centred Gold Complexes. *Chem. Soc. Rev.* **2008**, *37*, 1952–1966.

5. He, X.; Yam, V. W.-W. Luminescent Gold(I) Complexes for Chemosensing. *Coord. Chem. Rev.* **2011**, *255*, 2111–2123.
6. Katz, M. J.; Sakai, K.; Leznoff, D. B. The Use of Auophilic and Other Metal-Metal Interactions as Crystal Engineering Design Elements to Increase Structural Dimensionality. *Chem. Soc. Rev.* **2008**, *37*, 1884–1895.
7. Puddephatt, R. J. Coordination Polymers: Polymers, Rings and Oligomers Containing Gold(I) Centres. *Coord. Chem. Rev.* **2001**, *216*, 313–332.
8. Puddephatt, R. J. Macrocycles, Catenanes, Oligomers and Polymers in Gold Chemistry. *Chem. Soc. Rev.* **2008**, *37*, 2012–2027.
9. Schmidbaur, H. Ludwig Mond Lecture. High-Carat Gold Compounds. *Chem. Soc. Rev.* **1995**, *24*, 391–400.
10. Schmidbaur, H.; Schier, A. A Briefing on Auophilicity. *Chem. Soc. Rev.* **2008**, *37*, 1931–1951.
11. Schmidbaur, H.; Schier, A. Auophilic Interactions as a Subject of Current Research: An Up-Date. *Chem. Soc. Rev.* **2012**, *41*, 370–412.
12. Yam, V. W.-W.; Lo, K. K.-W. Luminescent Polynuclear d<sup>10</sup> Metal Complexes. *Chem. Soc. Rev.* **1999**, *28*, 323–334.
13. Yam, V. W.-W.; Au, V. K.-M.; Leung, S. Y.-L. Light-Emitting Self-Assembled Materials Based on d<sup>8</sup> and d<sup>10</sup> Transition Metal Complexes. *Chem. Rev.* **2015**, *115*, 7589–7728.
14. Yam, V. W.-W.; Cheng, E. C.-C. Highlights on the Recent Advances in Gold Chemistry—A Photophysical Perspective. *Chem. Soc. Rev.* **2008**, *37*, 1806–1813.
15. Yam, V. W.-W.; Cheng, E. C.-C. Molecular Gold–Multinuclear Gold(I) Complexes. *Angew. Chem. Int. Ed.* **2000**, *39*, 4240–4242.
16. Balch, A. L.; Olmstead, M. M.; Vickery, J. C. Gold(I) Compounds without Significant Auophilic Intermolecular Interactions: Synthesis, Structure, and Electronic Properties of Ph<sub>3</sub>PAuC(O)NHMe and Au<sub>3</sub>(PhCH<sub>2</sub>NCOMe)<sub>3</sub>: Comparative Monomeric and Trimeric Analogues of the Solvoluminescent Trimer, Au<sub>3</sub>(MeNCOMe)<sub>3</sub>. *Inorg. Chem.* **1999**, *38*, 3494–3499.
17. Brandys, M. C.; Puddephatt, R. J. Strongly Luminescent Three-Coordinate Gold(I) Polymers: 1D Chain-Link Fence and 2D Chickenwire Structures. *J. Am. Chem. Soc.* **2001**, *123*, 4839–4840.
18. Canales, F.; Gimeno, M. C.; Laguna, A.; Jones, P. G. Auophilicity at Sulfur Centers. Synthesis and Reactivity of the Complex [S(Au<sub>2</sub>dppf)]; Formation of Polynuclear Sulfur-Centered Complexes. Crystal Structures of [S(Au<sub>2</sub>dppf)]·2CHCl<sub>3</sub>, [(μ-Au<sub>2</sub>dppf){S(Au<sub>2</sub>dppf)}<sub>2</sub>]·(OTf)<sub>2</sub>·8CHCl<sub>3</sub>, and [S(AuPPh<sub>2</sub>Me)<sub>2</sub>(Au<sub>2</sub>dppf)]·(ClO<sub>4</sub>)<sub>2</sub>·3CH<sub>2</sub>Cl<sub>2</sub>. *J. Am. Chem. Soc.* **1996**, *118*, 4839–4845.
19. Chen, J.; Mohamed, A. A.; Abdou, H. E.; Krause Bauer, J. A.; Fackler, J. J. P.; Bruce, A. E.; Bruce, M. R. M. Novel Metallamacrocyclic Gold(I) Thiolate Cluster Complex: Structure and Luminescence of [Au<sub>9</sub>(μ-dppm)<sub>4</sub>(μ-p-tc)<sub>6</sub>](PF<sub>6</sub>)<sub>3</sub>. *Chem. Commun.* **2005**, *12*, 1575–1577.
20. Chui, S. S.-Y.; Chen, R.; Che, C.-M. A Chiral [2]Catenane Precursor of the Antiarthritic Gold(I) Drug Auranofin. *Angew. Chem. Int. Ed.* **2006**, *45*, 1621–1624.
21. Fenske, D.; Langetepe, T.; Kappes, M. M.; Hampe, O.; Weis, P. Selenium-Bridged Gold(I) Complex Cations [Au<sub>10</sub>Se<sub>4</sub>(dppm)<sub>4</sub>]<sup>2+</sup> and [Au<sub>18</sub>Se<sub>8</sub>(dppe)<sub>6</sub>]<sup>2+</sup>. *Angew. Chem. Int. Ed.* **2000**, *39*, 1857–1860.
22. Fung, E. Y.; Olmstead, M. M.; Vickery, J. C.; Balch, A. L. Glowing Gold Rings: Solvoluminescence from Planar Trigold(I) Complexes. *Coord. Chem. Rev.* **1998**, *171*, 151–159.
23. Jia, J.-H.; Wang, Q.-M. Intensely Luminescent Gold(I)-Silver(I) Cluster with Hypercoordinated Carbon. *J. Am. Chem. Soc.* **2009**, *131*, 16634–16635.
24. Jiang, X.-F.; Hau, F. K.-W.; Sun, Q.-F.; Yu, S.-Y.; Yam, V. W.-W. From {AuI...AuI}-Coupled Cages to the Cage-Built 2-D {AuI...AuI} Arrays: AuI...AuI Bonding Interaction Driven Self-Assembly and Their AgI Sensing and Photo-Switchable Behavior. *J. Am. Chem. Soc.* **2014**, *136*, 10921–10929.
25. Kemper, B.; Zengerling, L.; Spitzer, D.; Otter, R.; Bauer, T.; Besenius, P. Kinetically Controlled Stepwise Self-Assembly of Au(I)-Metallopeptides in Water. *J. Am. Chem. Soc.* **2018**, *140*, 534–537.
26. Koshevoy, I. O.; Chang, Y.-C.; Karttunen, A. J.; Haukka, M.; Pakkanen, T.; Chou, P.-T. Modulation of Metallophilic Bonds: Solvent-Induced Isomerization and Luminescence Vapochromism of a Polymorphic Au–Cu Cluster. *J. Am. Chem. Soc.* **2012**, *134*, 6564–6567.
27. Lasanta, T.; Olmos, M. E.; Laguna, A.; López-de-Luzuriaga, J. M.; Naumov, P. Making the Golden Connection: Reversible Mechanochemical and Vapochemical Switching of Luminescence from Bimetallic Gold–Silver Clusters Associated through Auophilic Interactions. *J. Am. Chem. Soc.* **2011**, *133*, 16358–16361.
28. Lee, Y.-A.; Eisenberg, R. Luminescence Tribochromism and Bright Emission in Gold(I) Thiouracilate Complexes. *J. Am. Chem. Soc.* **2003**, *125*, 7778–7779.
29. Lim, S. H.; Olmstead, M. M.; Balch, A. L. Molecular Accordion: Vapoluminescence and Molecular Flexibility in the Orange and Green Luminescent Crystals of the Dimer, Au<sub>2</sub>(μ-bis-(diphenylphosphino)ethane)<sub>2</sub>Br<sub>2</sub>. *J. Am. Chem. Soc.* **2011**, *133*, 10229–10238.
30. Lim, S. H.; Olmstead, M. M.; Balch, A. L. Inorganic Topochemistry. Vapor-Induced Solid State Transformations of Luminescent, Three-Coordinate Gold(I) Complexes. *Chem. Sci.* **2013**, *4*, 311–318.
31. Liu, Q.; Xie, M.; Chang, X.; Cao, S.; Zou, C.; Fu, W.-F.; Che, C.-M.; Chen, Y.; Lu, W. Tunable Multicolor Phosphorescence of Crystalline Polymeric Complex Salts with Metallophilic Backbones. *Angew. Chem. Int. Ed.* **2018**, *57*, 6279–6283.
32. Manbeck, G. F.; Brennessel, W. W.; Stockland, R. A.; Eisenberg, R. Luminescent Au(I)/Cu(I) Alkynyl Clusters with an Ethynyl Steroid and Related Aliphatic Ligands: An Octanuclear Au<sub>4</sub>Cu<sub>4</sub> Cluster and Luminescence Polymorphism in Au<sub>3</sub>Cu<sub>2</sub> Clusters. *J. Am. Chem. Soc.* **2010**, *132*, 12307–12318.
33. Mansour, M. A.; Connick, W. B.; Lachicotte, R. J.; Gysling, H. J.; Eisenberg, R. Linear Chain Au(I) Dimer Compounds as Environmental Sensors: A Luminescent Switch for the Detection of Volatile Organic Compounds. *J. Am. Chem. Soc.* **1998**, *120*, 1329–1330.
34. Mingos, D. M. P.; Yau, J.; Menzer, S.; Williams, D. J. A Gold(I) [2]Catene. *Angew. Chem. Int. Ed.* **1995**, *34*, 1894–1895.

35. Ni, W.-X.; Li, M.; Zheng, J.; Zhan, S.-Z.; Qiu, Y.-M.; Ng, S. W.; Li, D. Approaching White-Light Emission from a Phosphorescent Trinuclear Gold(I) Cluster by Modulating Its Aggregation Behavior. *Angew. Chem. Int. Ed.* **2013**, *52*, 13472–13476.
36. Polgar, A. M.; Weigend, F.; Zhang, A.; Stillman, M. J.; Corrigan, J. F. A N-Heterocyclic Carbene-Stabilized Coinage Metal-Chalcogenide Framework with Tunable Optical Properties. *J. Am. Chem. Soc.* **2017**, *139*, 14045–14048.
37. Rawashdeh-Omary, M. A.; Omary, M. A.; Fackler, J. P.; Galassi, R.; Pietroni, B. R.; Burini, A. Chemistry and Optoelectronic Properties of Stacked Supramolecular Entities of Trinuclear Gold(I) Complexes Sandwiching Small Organic Acids. *J. Am. Chem. Soc.* **2001**, *123*, 9689–9691.
38. Scherbaum, F.; Grohmann, A.; Huber, B.; Krüger, C.; Schmidbaur, H. “Auophilicity” as a Consequence of Relativistic Effects: The Hexakis(triphenylphosphaneaurio)methane Dication  $[(\text{Ph}_3\text{PAu})_6\text{C}]^{2+}$ . *Angew. Chem. Int. Ed.* **1988**, *27*, 1544–1546.
39. Sevillano, P.; Langetepe, T.; Fenske, D. Neue Gold-Selen-Komplexverbindungen: Synthesen und Strukturen von  $[\text{Au}_{10}\text{Se}_4(\text{dpppe})_4]\text{Br}_2$ ,  $[\text{Au}_2\text{Se}(\text{dppbe})]_{\infty}$ ,  $[(\text{Au}_3\text{Se}_2(\text{dppbp})_3]\text{Cl}_2$  and  $[\text{Au}_{34}\text{Se}_{14}(\text{tpep})_6(\text{tpepSe})_2]\text{Cl}_6$ . *Z. Anorg. Allg. Chem.* **2003**, *629*, 207–214.
40. Shakirova, J. R.; Grachova, E. V.; Sizov, V. V.; Starova, G. L.; Koshevoy, I. O.; Melnikov, A. S.; Gimeno, M. C.; Laguna, A.; Tunik, S. P. Polynuclear Cage-Like Au(I) Phosphane Complexes Based on a  $\text{S}^{2-}$  Template: Observation of Multiple Luminescence in Coordinated Polyaromatic Systems. *Dalton Trans.* **2017**, *46*, 2516–2523.
41. Siemeling, U.; Rother, D.; Bruhn, C.; Fink, H.; Weidner, T.; Träger, F.; Rothenberger, A.; Fenske, D.; Priebe, A.; Maurer, J.; Winter, R. The Interaction of 1,1'-Diisocyanoferrocene with Gold: Formation of Monolayers and Supramolecular Polymerization of an Auophilic Ferrocenophane. *J. Am. Chem. Soc.* **2005**, *127*, 1102–1103.
42. Sun, Q.-F.; Lee, T. K.-M.; Li, P.-Z.; Yao, L.-Y.; Huang, J.-J.; Huang, J.; Yu, S.-Y.; Li, Y.-Z.; Cheng, E. C.-C.; Yam, V. W.-W. Self-Assembly of a Neutral Luminescent  $\text{Au}_{12}$  Cluster with  $\text{D}_2$  Symmetry. *Chem. Commun.* **2008**, *43*, 5514–5516.
43. Wang, Q.-M.; Lee, Y.-A.; Crespo, O.; Deaton, J.; Tang, C.; Gysling, H. J.; Concepción Gimeno, M.; Larraz, C.; Villacampa, M. D.; Laguna, A.; Eisenberg, R. Intensely Luminescent Gold(I)-Silver(I) Cluster Complexes with Tunable Structural Features. *J. Am. Chem. Soc.* **2004**, *126*, 9488–9489.
44. Yip, S.-K.; Cheng, E. C.-C.; Yuan, L.-H.; Zhu, N.; Yam, V. W.-W. Supramolecular Assembly of Luminescent Gold(I) Alkynylcalix[4]crown-6 Complexes with Planar  $\eta^2,\eta^2$  Coordinated Gold(I) Centers. *Angew. Chem. Int. Ed.* **2004**, *43*, 4954–4957.
45. Yu, S.-Y.; Sun, Q.-F.; Lee, T. K.-M.; Cheng, E. C.-C.; Li, Y.-Z.; Yam, V. W.-W.  $\text{Au}_{36}$  Crown: A Macrocyclization Directed by Metal-Metal Bonding Interactions. *Angew. Chem. Int. Ed.* **2008**, *47*, 4551–4554.
46. Yu, S.-Y.; Zhang, Z.-X.; Cheng, E. C.-C.; Li, Y.-Z.; Yam, V. W.-W.; Huang, H.-P.; Zhang, R. A Chiral Luminescent  $\text{Au}_{16}$  Ring Self-Assembled from Achiral Components. *J. Am. Chem. Soc.* **2005**, *127*, 17994–17995.
47. Zeller, E.; Beruda, H.; Kolb, A.; Bissinger, P.; Riede, J.; Schmidbaur, H. Change of Coordination from Tetrahedral Gold-Ammonium to Square-Pyramidal Gold-Arsenium Cations. *Nature* **1991**, *352*, 141–143.
48. Cheng, E. C.-C.; Lo, W.-Y.; Lee, T. K.-M.; Zhu, N.; Yam, V. W.-W. Synthesis, Characterization, and Luminescence Studies of Discrete Polynuclear Gold(I) Sulfido and Selenido Complexes with Intramolecular Auophilic Contacts. *Inorg. Chem.* **2014**, *53*, 3854–3863.
49. Hau, F. K.-W.; Lee, T. K.-M.; Cheng, E. C.-C.; Au, V. K.-M.; Yam, V. W.-W. Luminescence Color Switching of Supramolecular Assemblies of Discrete Molecular Decanuclear Gold(I) Sulfido Complexes. *Proc. Natl. Acad. Sci. U. S. A.* **2014**, *111*, 15900–15905.
50. Yao, L.-Y.; Low, K.-H.; Yam, V. W.-W. A Gold Quartet Framework with Reversible Anisotropic Structural Transformation Accompanied by Luminescence Response. *Chem* **2019**, *5*, 2418–2428.
51. Lee, T. K.-M.; Zhu, N.; Yam, V. W.-W. An Unprecedented Luminescent Polynuclear Gold(I)  $\mu_3$ -Sulfido Cluster With a Thiacrown-Like Architecture. *J. Am. Chem. Soc.* **2010**, *132*, 17646–17648.
52. Yam, V. W.-W.; Cheng, E. C.-C.; Cheung, K.-K. A Novel High-Nuclearity Luminescent Gold(I)-Sulfido Complex. *Angew. Chem. Int. Ed.* **1999**, *38*, 197–199.
53. Yam, V. W.-W.; Cheng, E. C.-C.; Zhou, Z.-Y. A Highly Soluble Luminescent Decanuclear Gold(I) Complex with a Propeller-Shaped Structure. *Angew. Chem. Int. Ed.* **2000**, *39*, 1683–1685.
54. Yao, L.-Y.; Hau, F. K.-W.; Yam, V. W.-W. Addition Reaction-Induced Cluster-to-Cluster Transformation: Controlled Self-Assembly of Luminescent Polynuclear Gold(I)  $\mu_3$ -Sulfido Clusters. *J. Am. Chem. Soc.* **2014**, *136*, 10801–10806.
55. Yao, L.-Y.; Lee, T. K.-M.; Yam, V. W.-W. Thermodynamic-Driven Self-Assembly: Heterochiral Self-Sorting and Structural Reconfiguration in Gold(I)-Sulfido Cluster System. *J. Am. Chem. Soc.* **2016**, *138*, 7260–7263.
56. Yao, L.-Y.; Yam, V. W.-W. Photoinduced Isomerization-Driven Structural Transformation Between Decanuclear and Octadecanuclear Gold(I) Sulfido Clusters. *J. Am. Chem. Soc.* **2015**, *137*, 3506–3509.
57. Li, K.; Cheng, G.; Ma, C.; Guan, X.; Kwok, W.-M.; Chen, Y.; Lu, W.; Che, C.-M. Light-Emitting Platinum(II) Complexes Supported by Tetradentate Dianionic Bis(N-heterocyclic carbene) Ligands: Towards Robust Blue Electrophosphors. *Chem. Sci.* **2013**, *4*, 2630–2644.
58. Li, K.; Ming Tong, G. S.; Wan, Q.; Cheng, G.; Tong, W.-Y.; Ang, W.-H.; Kwong, W.-L.; Che, C.-M. Highly Phosphorescent Platinum(II) Emitters: Photophysics, Materials and Biological Applications. *Chem. Sci.* **2016**, *7*, 1653–1673.
59. Lu, G.-H.; Li, L.-G.; Yang, X.-N. Achieving Perpendicular Alignment of Rigid Polythiophene Backbones to the Substrate by Using Solvent-Vapor Treatment. *Adv. Mater.* **2007**, *19*, 3594–3598.
60. Park, S. H.; Jin, Y.; Kim, J. Y.; Kim, S. H.; Kim, J.; Suh, H.; Lee, K. A Blue-Light-Emitting Polymer with a Rigid Backbone for Enhanced Color Stability. *Adv. Funct. Mater.* **2007**, *17*, 3063–3068.

61. Cheng, X.; Zhang, Q.; Xie, J.-H.; Wang, L.-X.; Zhou, Q.-L. Highly Rigid Diphosphane Ligands with a Large Dihedral Angle Based on a Chiral Spirobifluorene Backbone. *Angew. Chem. Int. Ed.* **2005**, *44*, 1118–1121.
62. Fan, C.; Duan, C.; Wei, Y.; Ding, D.; Xu, H.; Huang, W. Dibenzothiophene-Based Phosphine Oxide Host and Electron-Transporting Materials for Efficient Blue Thermally Activated Delayed Fluorescence Diodes through Compatibility Optimization. *Chem. Mater.* **2015**, *27*, 5131–5140.
63. Chan, A. K.-W.; Ng, M.; Low, K.-H.; Yam, V. W.-W. Versatile Control of Directed Supramolecular Assembly via Subtle Changes of the Rhodium(I) Pincer Building Blocks. *J. Am. Chem. Soc.* **2018**, *140*, 8321–8329.
64. Keter, F. K.; Guzei, I. A.; Nell, M.; Zyl, W. E. v.; Darkwa, J. Phosphinogold(I) Dithiocarbamate Complexes: Effect of the Nature of Phosphine Ligand on Anticancer Properties. *Inorg. Chem.* **2014**, *53*, 2058–2067.
65. Chu, A.; Hau, F. K.-W.; Yao, L.-Y.; Yam, V. W.-W. Decanuclear Gold(I) Sulfido Pseudopolymorphs Displaying Stimuli-Responsive RGBY Luminescence Changes. *ACS Mater. Lett.* **2019**, *1*, 277–284.
66. Yam, V. W.-W.; Lai, T.-F.; Che, C.-M. Novel Luminescent Polynuclear Gold(I) Phosphine Complexes. Synthesis, Spectroscopy, and X-ray Crystal Structure of  $[Au_3(dmmp)_2]^{3+}$  [ $dmmp = \text{bis}(\text{dimethylphosphinomethyl})\text{methylphosphine}$ ]. *J. Chem. Soc. Dalton Trans.* **1990**, *38*, 3747–3752.
67. Yam, V. W.-W.; Lee, W.-K. Synthesis, Spectroscopy and Excited-State Redox Properties of Novel Luminescent Trinuclear Three-Co-Ordinate Gold(I) Phosphine Complexes. *J. Chem. Soc. Dalton Trans.* **1993**, *22*, 2097–2100.